High pressure study on induced S$_A$ phases in binary liquid crystal mixtures

G. Illian[a]; H. Kneppe[a]; F. Schneider[a]

[a] Physikalische Chemie, Universität Siegen, Siegen, F. R. Germany

PLEASE SCROLL DOWN FOR ARTICLE

High pressure study on induced S_A phases in binary liquid crystal mixtures

by G. ILLIAN, H. KNEPPE and F. SCHNEIDER

Physikalische Chemie, Universität Siegen, 5900 Siegen, F.R. Germany

Binary mixtures of terminal polar and non-polar liquid crystals exhibiting induced smectic phases are studied under high pressure. For terminal polar compounds with smectic phases, there are two types of T, x phase diagrams known up to now. Diagrams with a nematic gap between the induced phase and the smectic phase of the terminal polar compound and diagrams with an uninterrupted miscibility of the smectic phases. We find a continuous transformation between these phase diagrams with pressure. At a certain pressure, the phase transition lines form a cross separating two nematic and two smectic phases.

1. Introduction

Mixtures of terminal polar and non-polar liquid crystals usually show phase diagrams with a very stable smectic phase (induced smectic phase) of the orthogonal type in the range of medium concentrations [1, 2]. If the pure terminal polar component also exhibits a smectic phase, two different types of phase diagram can be observed which are shown schematically in figures 1 and 2. An uninterrupted miscibility of the induced S_A phase and the S_A phase of the polar component (see figure 1) is usually found in mixtures of 4-n-octyloxy-4'-cyanobiphenyl (8OCB) with terminal non-polar esters having long alkyl chains. Esters with short alkyl chains usually exhibit phase diagrams with a nematic gap [3] between the two smectic phases (see figure 2). On both sides of the nematic gap, the reentrant phenomenon, i.e. the phase sequence N_{re}–S_A–N, is observed. The question arises as to whether these two types of phase diagram are principally different. Such a principal difference could be caused by slight differences in the layer structure which is, in fact, different: a monolayer (S_{A_1}) for the induced phase [3, 4] and a bilayer (S_{A_d}) structure for the pure polar component [5].

A hint that both types of phase diagram can be transformed into one another is given by the phase diagram for 4-n-butyloxyphenyl-4'-n-pentyloxybenzoate and 8OCB [6]. This phase diagram shows besides the maximum of the induced S_A phase a minimum in the phase boundary line N–S_A on the 8OCB side.

It is known that the application of pressure reduces the stability of the S_{A_d} phase [7], whereas nearly all other liquid crystal phases are stabilized. Therefore, it is possible to change significantly the form of a phase diagram with an induced smectic phase by application of pressure. We have now tried to find the missing link between the different types of phase diagram with induced smectic phases by studying suitable binary systems under high pressure.

2. Experimental

Phase transition temperatures were determined in a polarizing microscope equipped with a high pressure autoclave. The sample holder is a further development of that

Figure 1. Schematic phase diagram of a binary mixture showing an uninterrupted miscibility of the induced S_A phase and the S_A phase of the pure component B. Biphasic regions between the liquid crystal phases are not shown. Dashed lines denote monotropic transitions.
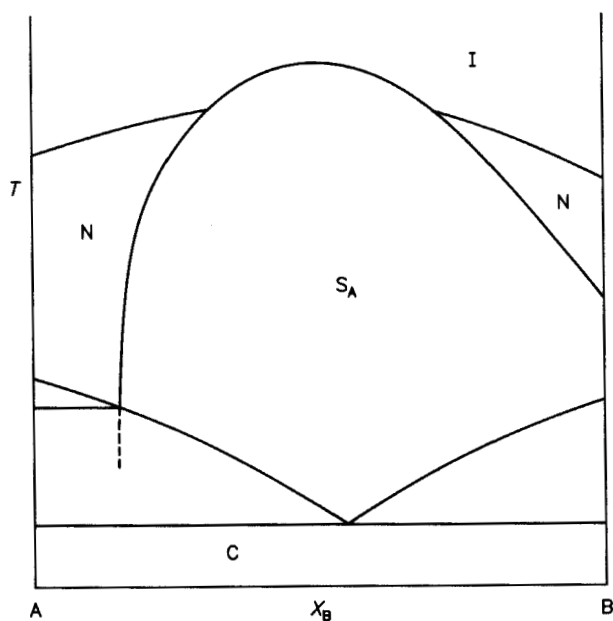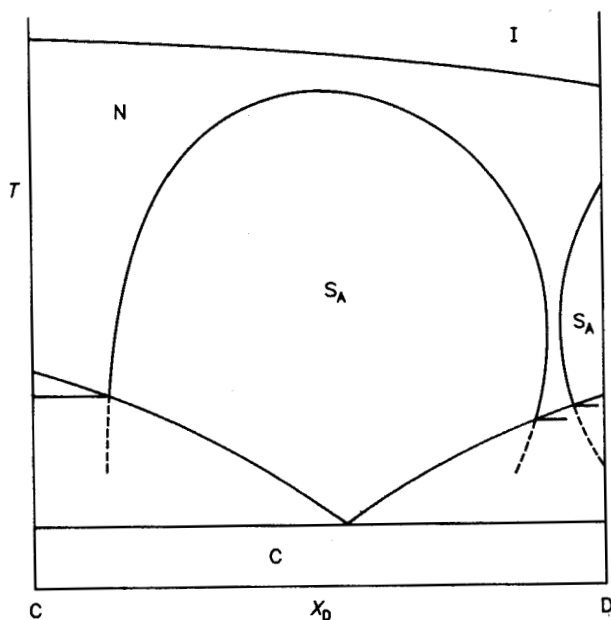

Figure 2. Schematic phase diagram of a binary mixture showing a nematic gap between the induced S_A phase and the S_A phase of the pure component D.
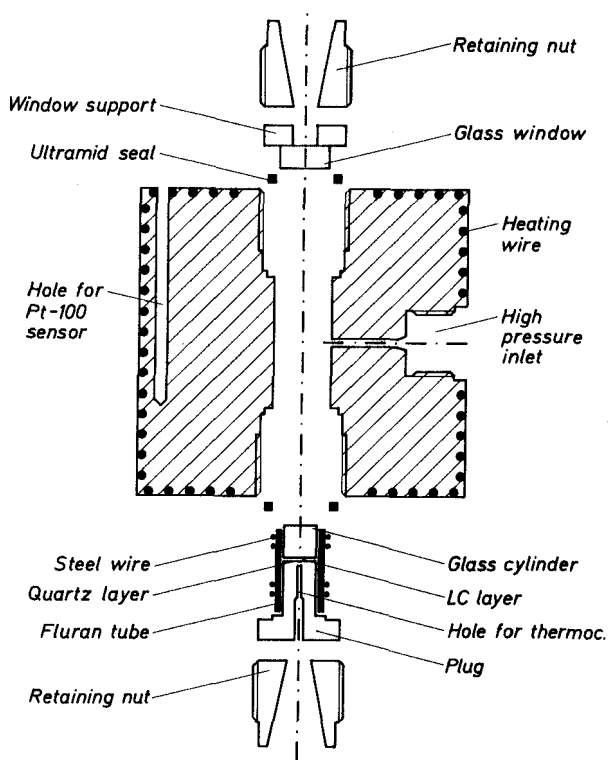
Figure 3. Schematic diagram of the high pressure cell.

of Keyes [8] and Shashidhar [9]. These sample holders show a strong delay between the sample temperature and that of the autoclave during temperature changes. This leads to limitations in the heating and cooling rate of the autoclave if reliable transition temperatures are to be determined. High rates are, however, favourable for the observation of phase transitions with minor texture changes and favourable for the study of monotropic transitions. In our design (see figure 3), the lower autoclave plug is used as the sample holder. The upper part of the sample holder is a glass or sapphire cylinder as in the design by Keyes and Shashidhar. Both parts are connected by a short piece of Fluran tube. The temperature of the sample is measured by means of a thermocouple (Thermocoax, Philips, 0·5 mm diameter) placed 0·5 mm below the sample. The temperature delay is only 0·04 K for a heating rate of 1 K/min.

As the sample illumination and observation is only possible from above, we have used a polarizing microscope with incident light (Wild, macroscope M420). If the liquid crystal to be studied is put directly on the polished steel plug, homeotropic alignment of the liquid crystal usually prevents the observation of phase transitions. Coatings with other metals led only to minor changes. A quartz coating (Liquicoat Si, Merck AG) which is fired at 120°C leads to a non-homeotropic alignment of the liquid crystal. The recommended firing temperature of 450°C leads to a more stable coating, but the tendency to form homeotropic textures increases. Finally, a very thin coating with aluminium gives sufficient reflectivity and retains the non-homeotropic alignment.

Air bubbles which would be dissolved in the liquid crystal under high pressure are removed under vacuum and by flushing with argon. This sample preparation gives

good results for the liquid crystals studied. Some chemically unstable liquid crystals, e.g. azomethins, show a deterioration in contact with the steel surface through micro holes in the quartz layer. Other metals, like gold or chromium, show nearly the same deterioration rate. In this case, the plug surface had to be coated with a thicker non-metallic layer, e.g. by coating with glass solder having a suitable thermal expansion coefficient.

The autoclave is made from maraging steel 1.6358 and designed to withstand a maximum pressure of 4 kbar. The maximum temperature is determined by the stability of the fluran tube. At 170°C, we observe a decrease of the clearing temperature of the liquid crystals. At lower temperatures, the clearing temperature is also lowered slowly by the diffusion of the softener from the Fluran tube. In the meantime, we use a special Fluran quality with a low softener content.

Pressure is generated by means of a piston screw pump and transmitted to the autoclave by paraffin oil. It is measured with several Bourdon gauges (0·1 per cent, WIKA) with different ranges.

The liquid crystals used were 4-*n*-heptyloxy-4′-cyanobiphenyl (7OCB, T_{NI} = 74·0°C), 4-*n*-nonyloxy-4′-cyanobiphenyl (9OCB, T_{NI} = 80·0°C) and 4-*n*-octyloxy-phenyl-4′-*n*-propyloxybenzoate ($\bar{3}$.O.$\bar{8}$, T_{NI} = 79·7°C). The two cyanobiphenyls were commercial products of BDH Ltd, the ester was synthesized by us. We use the acronym MCB for a mixture of 65 mole per cent 7OCB and 35 mole per cent 9OCB.

3. Results

A favourable candidate for the terminal polar component is 8OCB. 7OCB exhibits no smectic phase and the smectic phase of 9OCB is very stable against application of pressure. In order to be able to measure the phase boundaries at low temperatures we have, however, not used 8OCB but depressed the melting point by using a mixture (MCB) of 7OCB (65 mole per cent) and 9OCB (35 mole per cent) which exhibits nearly the same properties as 8OCB apart from the melting point. For the terminal non-polar component, we have used esters which are rather stable and show uninterrupted miscibility as well as a nematic gap depending on the length of the alkyl chain. $\bar{3}$.O.$\bar{8}$ has a medium chain length and the phase diagram (see figure 4) with MCB shows the induced S_A phase and a slight minimum at high MCB concentrations. Very small biphasic regions which are not shown in the figures were observed for the transition nematic–isotropic and for the transition smectic–nematic at low MCB concentrations. No biphasic regions were detected at high MCB concentrations. Application of pressure (see figures 5–9) shows that a reentrant nematic phase is stabilized by pressure and at about 1010 bar the S_A–N_{re} phase boundary meets the N–S_A line. The temperature of this invariant point, which we call the crossing point, is 54°C and the concentration x_{MCB} is 0·90. The measurements suggest that the course of the phase boundary around this crossing point is like a cross. However, other courses are also possible and the precision of the measurements is not sufficient to exclude these; this point is discussed in the next section. At higher pressures a nematic gap appears and finally the S_A phase on the polar side of the phase diagram disappears.

Figure 10 shows the maximum pressure at which an S_A phase can be observed as a function of concentration. The maximum pressure values were calculated from fits $p = f(T)$ to the experimental values for fixed concentrations. The minimum in this curve corresponds to the concentration at which the nematic gap appears. The finite maximum pressure at the MCB side shows the disappearance of this phase at about 1·6 kbar and the divergence of this curve for concentrations x_{MCB} of about 0·77
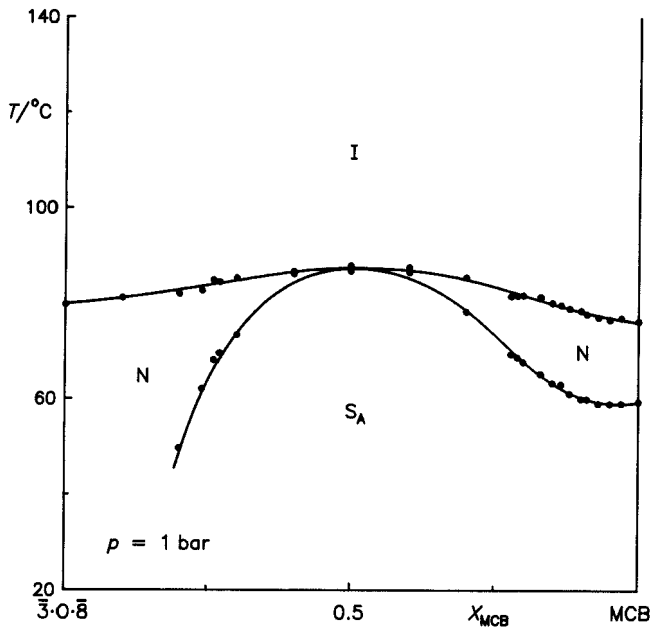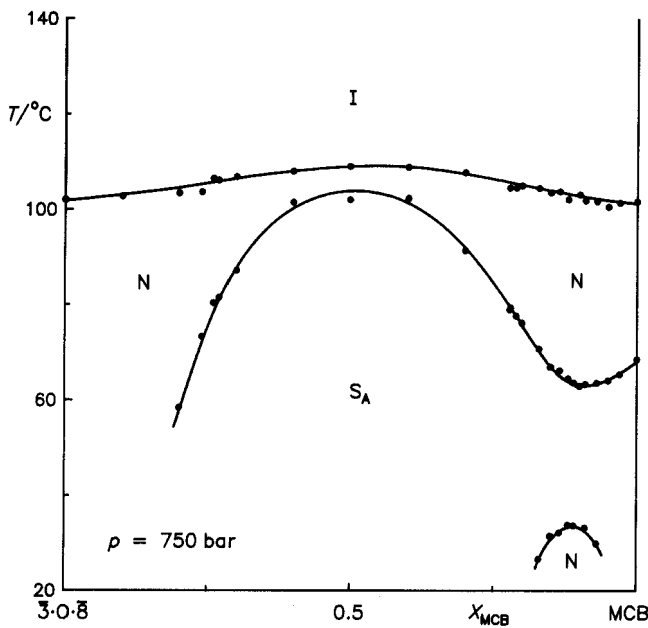
Figure 4.

Figure 5.

shows that the central part of the induced S_A phase is stable against application of pressure.

4. Discussion
The measurements show that the two types of phase diagram shown in figures 1 and 2 are extreme cases in a series of phase diagrams going from the uninterrupted
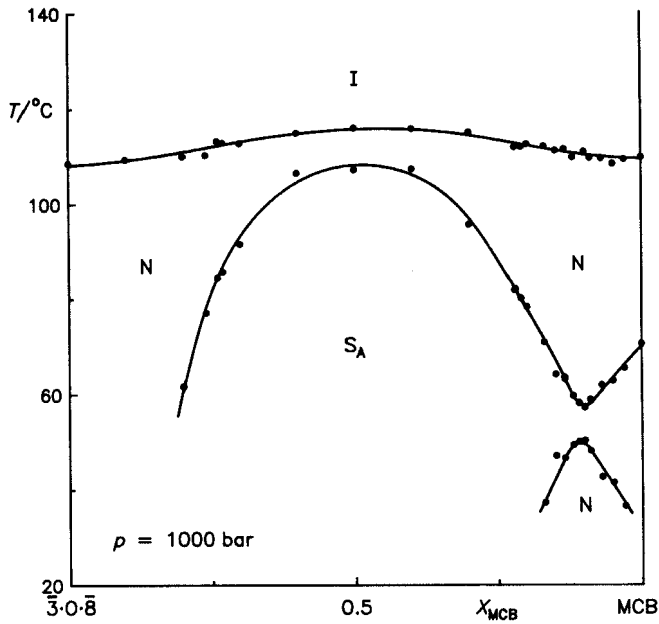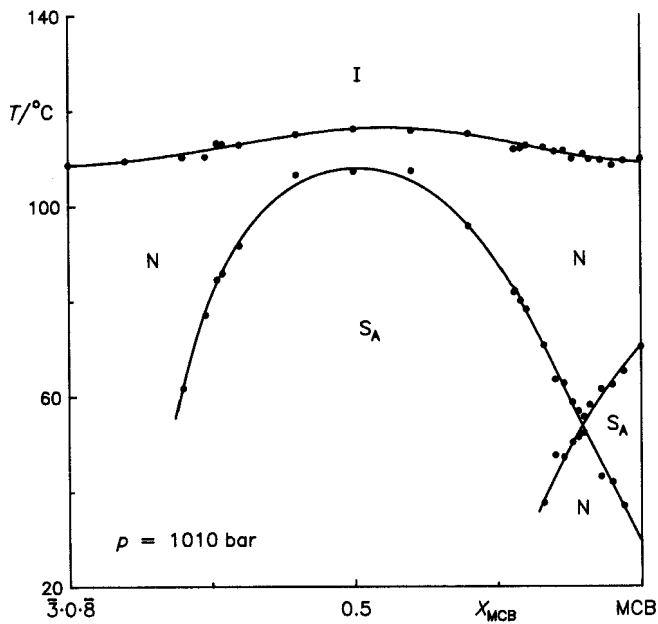
Figure 6.

Figure 7.

miscibility in the smectic phase to the nematic gap. The continuous transition between these two types of phase diagram produced by application of pressure suggests that this crossing point can also be found in phase diagrams at atmospheric pressure using a special ester mixture.

The transition between the two types of phase diagram is very interesting as such a transition is unknown up to know. However Prost and Toner [14] have predicted
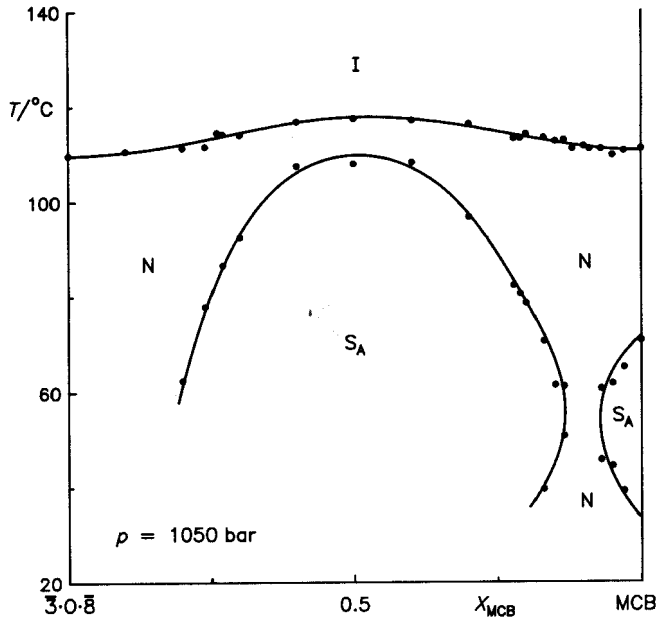
Figure 8.
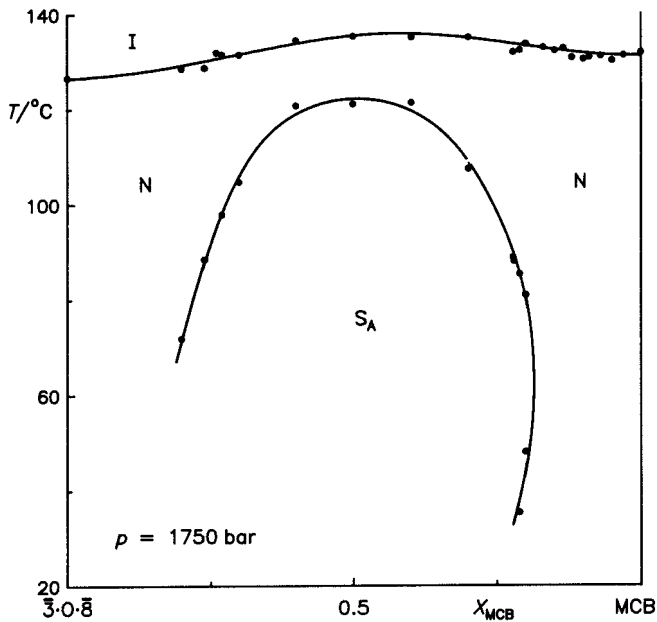
Figure 4–9. Phase diagrams for $\overline{3}.O.\overline{8}$/MCB mixtures at different pressures. Solid phases are not shown.

such a phase diagram with a dislocation-loop melting theory. According to this theory, one of the nematic phases is caused by fluctuations in the vicinity of a S_{A_1}–S_{A_d} critical point. The nematic phases of our system, however, do not belong to this special type of phase.

Other measurements [15] and our observations suggest that the phase transitions around the crossing point should be nearly continuous. At least, we were not able

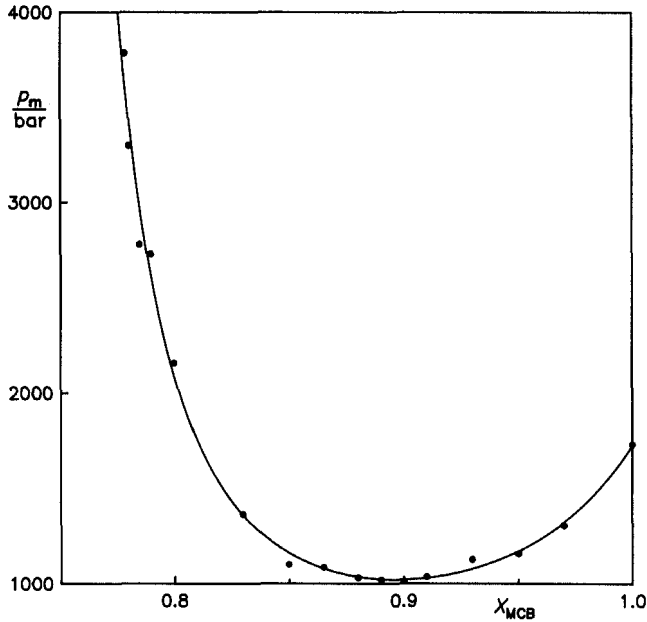Figure 10.   Maximum pressure p_m for a stable S_A phase in the binary mixture $\bar{3}.O.\bar{8}$/MCB as a function of concentration.

to observe biphasic regions. For continuous phase transitions, there must be a point at which an overcrossing of the two phases takes place. As this crossing point is invariant, the Gibbs phase rule demands four phases in equilibrium, which seems to be an artifact of the rule.

The precise course of the phase boundary around this crossing point cannot be evaluated from the measurements and so we have studied this problem using thermodynamics. We are only interested in the course of the phase boundary in the neighbourhood of the crossing point, i.e. the thermodynamic data of the two phases will only exhibit minor changes as a function of pressure, temperature, and concentration. In this case, the expansion of the Gibbs free energy [10, 11] around the crossing point or a point nearby up to second order will lead to a good description of the phases. As biphasic regions are missing or very small, we can use an equal G analysis for the calculation of the equilibrium [12]. This shortens the thermodynamic calculations considerably. This combination of an equal G analysis and an expansion has already been used to describe smectic–nematic phase transitions showing a closed loop phase boundary line [13].

The expansion of the molar free energy difference $\Delta G = G_S - G_N$ up to second order around a reference point p_0, T_0, x_0 leads to

$$\Delta G = A_0 + A_1 (T - T_0) + A_2 (p - p_0) + A_3 (x - x_0) + A_4 (T - T_0)^2$$
$$+ A_5 (p - p_0)^2 + A_6 (x - x_0)^2 + A_7 (T - T_0) (p - p_0)$$
$$+ A_8 (T - T_0) (x - x_0) + A_9 (p - p_0) (x - x_0), \tag{1}$$

where the coefficients A_i are the derivatives of ΔG with respect to p, T, x, e.g. $A_1 = (\partial \Delta G / \partial T)_0 = -\Delta S_0$. According to the equal G analysis, the equilibrium condition is

$$\Delta G = 0. \tag{2}$$

Equation (1) combined with equation (2) represents the equilibrium surface in three dimensions. In two dimensions, the equilibrium lines are sections of a cone, e.g. hyperbolas in the T, x plane. In our case, the main axis of the hyperbola is parallel to the T axis for low pressure and parallel to the x axis for high pressure. The transformation of these hyperbolas with different directions of the main axes into one another is only possible via a pair of straight lines in T, x space. Therefore, the linear terms in T and x and the term A_0 must disappear, if the reference point p_0, T_0, x_0 agrees with the crossing point p_c, T_c, x_c; giving

$$A_2 (p - p_c) + A_4 (T - T_c)^2 + A_5 (p - p_c)^2 + A_6 (x - x_c)^2$$
$$+ A_7 (T - T_c) (p - p_c) + A_8 (T - T_c) (x - x_c) + A_9 (p - p_c) (x - x_c) = 0. \tag{3}$$

Furthermore, equation (3) can be divided by one expansion coefficient. We have chosen the division by A_4, as the resultant equation

$$a_2 (p - p_c) + (T - T_c)^2 + a_5 (p - p_c)^2 + a_6 (x - x_c)^2 + a_7 (T - T_c) (p - p_c)$$
$$+ a_8 (T - T_c) (x - x_c) + a_9 (p - p_c) (x - x_c) = 0. \tag{4}$$

is usually solved for T in order to calculate T, x phase diagrams. The coefficients of this equation were fitted to the experimental data in the range $900 < p < 1100$ bar and $0.75 < x_{MCB} < 1$ (70 data points) using the Marquardt algorithm for an implicit function. Figure 11 shows the result calculated with the parameter set

$$a_2 = 0.5500 \, \text{bar}^{-1} \text{K}^2,$$

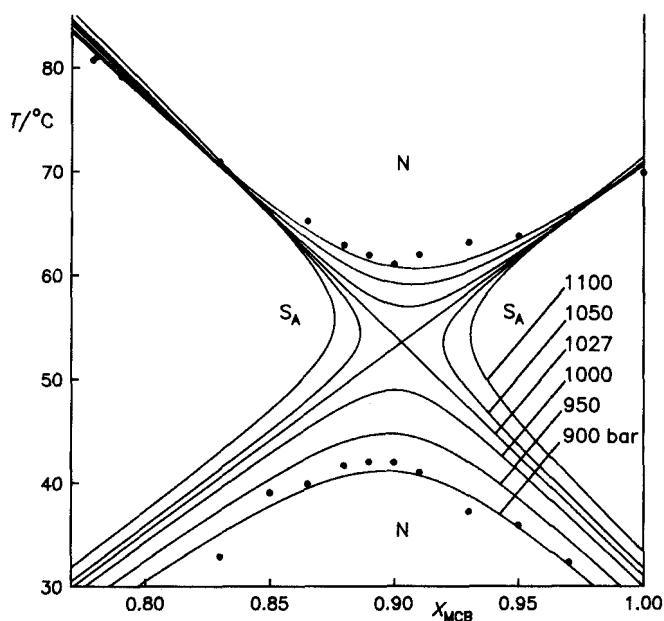$$a_5 = -0.001212 \, \text{bar}^{-2} \text{K}^2,$$

Figure 11. Phase boundary lines calculated with equation (4) using the parameter set given in the text. Full circles are measured values at a pressure of 900 bar. Further data points were not included for the sake of clarity of the figure.

$$a_6 = -41440\,\mathrm{K}^2,$$

$$a_7 = -0\!\cdot\!04169\,\mathrm{K\,bar}^{-1},$$

$$a_8 = 54\!\cdot\!71\,\mathrm{K},$$

$$a_9 = -0\!\cdot\!6704\,\mathrm{bar}^{-1}\,\mathrm{K}^2,$$

$$p_\mathrm{c} = 1027\,\mathrm{bar},$$

$$T_\mathrm{c} = 53\!\cdot\!52°\mathrm{C},$$

$$x_\mathrm{c} = 0\!\cdot\!9030$$

and the measured values for p of 900 bar. The apparent discrepancy between the assumed continuity of the phase transition and the parameter set which indicates a first order transition has been discussed in a recent paper [13]. The agreement between the 900 bar curve and the measured values is limited by the scatter of the measured values. The design of our high pressure cell and the sample preparation did not allow a higher precision. A measurement with a heating stage for atmospheric pressure on a system that shows this crossing point at atmospheric pressure would be very advantageous.

References

[1] DAVE, J. S., PATEL, P. R., and VASANTH, K. L., 1966, *Ind. J. Chem.*, **4**, 505.

[2] ENGELEN, B., HEPPKE, G., HOPF, R., and SCHNEIDER, F., 1978, *Ann. Phys.*, **3**, 403.

[3] ENGELEN, B., HEPPKE, G., HOPF, R., and SCHNEIDER, F., 1979, *Molec. Crystals liq. Crystals Lett.*, **49**, 193.

[4] ENGELEN, B., and SCHNEIDER, F., 1978, *Z. Naturf. (a)*, **33**, 1077.

[5] GRAY, G. W., and LYDON, J. E., 1974, *Nature, Lond.*, **252**, 221.

[6] SRIKANTA, B. S., and MADHUSUDANA, N. V., 1984, *Molec. Crystals liq. Crystals*, **108**, 39.

[7] CLADIS, P. E., BOGARDUS, R. K., DANIELS, W. B., and TAYLOR, G. N., 1977, *Phys. Rev. Lett.*, **11**, 720.

[8] KEYES, P. H., WESTON, H. T., and DANIELS, W. B., 1973, *Phys. Rev. Lett.*, **31**, 628.

[9] KALKURA, A. N., SHASHIDHAR, R., and SUBRAMANYA RAY URS, N., 1983, *J. Phys., Paris*, **44**, 51.

[10] CLARK, N. A., 1979, *J. Phys., Paris*, **40**, C3-345.

[11] KLUG, D. D., and WHALLEY, E., 1979, *J. chem. Phys.*, **71**, 1874.

[12] VAN HECKE, G. R., 1985, *J. phys. Chem.*, **89**, 2058.

[13] ILLIAN, G., KNEPPE, H., and SCHNEIDER, F., 1988, *Ber. Bunsenges. phys. Chem.*, **92**, 776.

[14] PROST, J., and TONER, J., 1987, *Phys. Rev. A*, **22**, 5008.

[15] KASTING, G. B., LUSHINGTON, K. J., and GARLAND, C. W., 1980, *Phys. Rev. B*, **22**, 321.